Anderton et al. Biointerphases 2013, 8:2
http://www.biointerphases.com/content/8/1/2

Biointerphases
a SpringerOpen Journal

ORIGINAL ARTICLE Open Access

The effect of high vacuum on the mechanical properties and bioactivity of collagen fibril matrices

Christopher R Anderton[1*], Frank W DelRio[1], Kiran Bhadriraju[2] and Anne L Plant[1]

Abstract

The extracellular matrix (ECM) environment plays a critical role in organism development and disease. Surface sensitive microscopy techniques for studying the structural and chemical properties of ECMs are often performed in high vacuum (HV) environments. In this report, we examine the affect HV conditions have on the bioactivity and mechanical properties of type I collagen fibrillar matrices. We find that HV exposure has an unappreciable affect on the cell spreading response and mechanical properties of these collagen fibril matrices. Conversely, low vacuum environments cause fibrils to become mechanically rigid as indicated by force microscopy, resulting in greater cell spreading. Time-of-flight secondary ion mass spectrometry results show no noticeable spectral differences between HV-treated and dehydrated matrices. While previous reports have shown that HV can denature proteins in monolayers, these observations indicate that HV-exposure does not mechanically or biochemically alter collagen in its supramolecular configuration. These results may have implication for complex ECM matrices such as decellularized scaffolds.

Keywords: Collagen fibrils, Extracellular matrix, Quantitative cell imaging, Colloidal probe atomic force microscopy, Secondary ion mass spectrometry, Principal component analysis

Background

Cellular interactions with the extracellular matrix (ECM) initiate an array of biophysical and biochemical signals that drive biological processes ranging from embryonic development to cancer progression [1-4]. In addition to receptor-mediated interactions between cells and the ECM [5,6], the mechanical environment that cells experience can exert strong influences on inter- and intracellular signaling and cell responses, and is likely critical to migration, differentiation, and development [4,7-10]. Elucidating the structural, mechanical, and chemical environment that the ECM presents to cells can be challenging. There has been a growing effort to employ a variety of surface sensitive microscopy techniques to measure the physicochemical properties of ECMs [11-16].

Recently, a number of reports have analyzed decellularized tissues and ECMs created by cells *in vitro* using electron, ion, and x-ray bombardment induced ionization microscopy methods, which are performed under high vacuum (HV) [13-15,17-22]. The use of scanning electron microscopy (SEM), for example, is commonplace for obtaining structural information of supramolecular ECM systems [13,17,18,20], but methods for accessing information about the chemical environment that the ECM provides to cells has been more elusive. Time-of-flight secondary ion mass spectrometry (ToF-SIMS) is one such technique that can provide chemical information about the surface of the material being analyzed. The ToF-SIMS sampling depth, when operated in a so-called static mode, is approximately 1 nm to 2 nm, rendering it ideal for determining the surface composition of complex protein samples [14,23-26]. ToF-SIMS data are conducive to a variety of multivariate analysis techniques, such as principal component analysis (PCA), to provide sensitive discrimination between parent molecules based on spectral differences [24,25]. For example, PCA with ToF-SIMS has been utilized for identifying and classifying a variety of biologically relevant samples such as sugars [27], lipids

* Correspondence: christopherranderton@gmail.com
[1]Material Measurement Laboratory, National Institute of Standards and Technology, Gaithersburg, MD 20899, USA
Full list of author information is available at the end of the article

[28,29], proteins [24-26], cell types [28,30], and decellularized or acellular ECMs [14,15,19,21].

The analysis of monomeric adsorbed protein films with ToF-SIMS has demonstrated that the HV environment can cause structural changes to these proteins [26]. These changes are indicated by spectral features, such as a more pronounced secondary ion yield from hydrophobic residues or a decrease or disappearance in yields from biochemical moieties that are hydrophilic or polar [26]. To prevent denaturation, it has been necessary to provide some mechanism to stabilize and preserve protein structure prior to analysis [23,26,31,32]. The potential sensitivity of proteins to HV denaturation could limit the usefulness of methods such as ToF-SIMS to provide data that are relevant to the *in vivo* ECM. With this in mind, it is important to elucidate whether any measurable biomechanical or biochemical changes from HV-exposure occur in complex supramolecular protein structures such as collagen fibrils.

Our group has previously developed a model ECM comprised of type I collagen, the most prevalent ECM protein, which self-assembles into matrices of fibrils [12,33,34]. These model matrices have a number of desirable properties that include: (i) collagen in a supramolecular structure that is more physiologically relevant than surface-adsorbed protein monomers [35], (ii) the ability to elicit robust and reproducible cell responses, (iii) excellent optical properties that facilitate quantifying cell response [12,33,34], and (iv) the means of systematically perturbing the chemical and/or mechanical properties [8,11,36,37]. These properties, coupled with the fact that collagen type I is the main component of connective tissue [13,38,39], make these fibril matrices an ideal model for studying how exposure to a HV environment may affect the physicochemical properties of supramolecular ECM structures. If the mechanical properties or chemistry of unfixed ECM materials are compromised by exposure to a HV environment, then application of techniques such as ToF-SIMS would require cumbersome and complicating preservation methods for maintaining physiologically relevant structures. However, if the affects from HV exposure were immeasurable, this would help to establish confidence in the use of HV methods for analysis of decellularized scaffolds.

Here, we analyze the effect of various treatments on the well-characterized model ECM of collagen type I fibrils to determine if exposure to a HV environment changes the bioactivity of these matrices, and consequently whether changes are due to differences in biochemical or biomechanical interactions. We have previously shown that passive dehydration of the collagen fibril matrices results in significantly increased spreading and proliferation, as well as other response differences, in NIH 3 T3 cells and vascular smooth muscle cells (A10 vSMCs) compared to cells on untreated fibril matrices [8,12,34,40,41]. The observed changes in cell response are due to mechanical stiffening of the fibril beds resulting from the dehydration process [11,12], as opposed to changes in integrin ligation [12,36,37]. Here, we examine the affect of HV exposure on fibrillar collagen by directly measuring the mechanical properties of the collagen with AFM, and also measuring biological response in the form of cell spreading. Furthermore, we look for differences in ToF-SIMS spectra of HV-treated and passively dehydrated matrices. We also compare HV treatment with low vacuum (LV) treatment, where the results suggest that conditions in slow removal of water may enhance stiffening of the fibrils due to capillary effects.

Methods

Disclaimer

Certain commercial products are identified in this report to adequately specify the experimental procedure. Such identification does not imply recommendation or endorsement by the National Institute of Standards and Technology, nor does it imply that the materials or equipment identified are necessarily the best available for the purpose.

Preparation of collagen fibril matrices

Type I collagen fibril matrices, which are composed of beds of ≈ 150 nm diameter fibrils that can extend to about ≈ 600 nm above the surface [34], were made as previously described [34,37]. Briefly, acid-stabilized collagen monomer solution (PureCol®, Advanced BioMatrix, Poway, CA) was diluted to 300 μg/mL using phosphate buffered saline (PBS, Invitrogen, Carlsbad, CA) and neutralized with sodium hydroxide (Sigma, St. Louis, MO). The resulting solution was incubated on gold-coated cover slips functionalized with 1-hexadecanethiol (Sigma) [34]. Alternatively, collagen solutions were incubated on 50 mm bacterial-grade polystyrene (PS) dishes (BD Falcon, Franklin Lakes, NJ) [33]. The samples were placed overnight at 37°C to facilitate collagen polymerization and fibril assembly on the surface. Excess collagen in solution was then aspirated from the sample, and the surface-adherent collagen was washed with PBS and de-ionized water. Following the washing steps, the matrices were exposed to a brief stream (10 s to 30 s) of filtered N_2 to remove the excess surface water from the fibril surface, which results in the creation of a bed of intersecting collagen fibrils. At this point, the fibril bed created is referred to as an untreated matrix. These matrices were stored in PBS at 4°C until further use [34]. Dehydrated collagen matrices were prepared identically to untreated ones, but prior to storage in PBS, they were left to passively dehydrate for 24 h in a laminar flow hood. After the

dehydration step they were then stored in PBS at 4°C until further use. To assess the effect that subsequent LV and HV exposure had on untreated fibrillar matrices, the untreated matrix samples were placed into a vacuum desiccator at 1 kPa to 10 kPa of pressure, or a ToF-SIMS sample chamber at 10^{-7} Pa to 10^{-8} Pa, respectively, for approximately 6 h. This time period was chosen because it is approximately the longest time the samples would experience these pressures for a HV-based analysis. On removal from the vacuum environments, the samples were placed in PBS and stored at 4°C until further use. All samples were stored in PBS at 4°C for no more than 36 h before they were analyzed.

Quantification of cell spreading

A10 rat vascular smooth muscle cells (ATCC (Manassas, VA) were cultured as previously described [34]. Briefly, cells were cultured in DMEM (Dulbecco's Modified Eagles Medium) obtained from Mediatech (Herndon, VA), supplemented with 10 (v/v) fetal bovine serum, non-essential amino acids, and glutamine at 4×10^{-3} mol/L (all from Gibco Invitrogen, Carlsbad, CA). Cells were maintained on tissue culture-treated polystyrene plates in a humidified incubator maintained at 5% CO_2 and 37°C and plated for experiments at a density of 1500 cells/cm^2. Cells were incubated on collagen fibril matrices for 24 h then rinsed with PBS, fixed with 4% paraformaldehyde in PBS, and permeabilized with 0.5% Triton X-100 in PBS. The fixed cells were stained with Texas Red maleimide (Sigma) to label the cell body and 4′, 6-diamidino-2-phenylindole (DAPI, Sigma) to label the cell nuclei as described previously [42]. Cells were then imaged on an Olympus IX70 inverted microscope (Olympus America, Melville, NY) equipped with a motorized stage for three dimensional position control, motorized filter wheels, and motorized shutters (Ludl Electronic Products, Hawthorne, NY) and controlled by IP Lab imaging software (BD, Exton, PA). Cell areas were then determined using a custom automated method with the Cell Morphology and Indicator Analysis Program, which is an ImageJ (National Institutes of Health, Bethesda, MD) plugin that thresholds and binarizes the fluorescence image data [42]. Analysis of resulting image data was performed in Excel (Microsoft, Redmond, WA) as described previously [12,36,37,42].

Atomic force microscopy (AFM) of fibril matrices

AFM of the collagen fibril matrices was performed on a MFP-3D-BIO AFM (Asylum Research, Santa Barbara, CA). All AFM measurements were performed at ambient temperature in PBS solution on collagen fibril beds formed on PS dishes, which behave similarly to fibril beds formed on thiolated Au films [33]. PS dishes were used here as the substrate in order to reduce sample preparation time, and because it is a convenient vessel for solution-phase AFM. This circumvented the need to transfer the samples to a secondary fluid cell, and insured that the samples stayed under buffered solution at all times. Topographical images were taken over 5 μm × 5 μm areas at a resolution of 512 pixels × 512 pixels using intermittent-contact mode at a linear scan rate of 0.18 Hz to 0.3 Hz with silicon nitride probes (k_{nom}= 0.03 N/m, BioLever, Olympus, Tokyo). Force microscopy measurements were carried out using the colloidal probe technique [11,43], which utilizes a microscale colloidal sphere as the probe tip, thereby allowing for mechanical property measurements over contact areas more similar to cell spread areas. In this study, commercially available AFM cantilevers with a gold colloidal sphere (sQube, Wetzlar, Germany) were used. Calibrating the colloidal probe cantilevers and conducting the force spectroscopy on each of the collagen fibril beds have been described previously [11]. Briefly, the colloidal probe cantilevers were calibrated by (i) determining the deflection sensitivity in air, (ii) measuring the spring constant (k) via the thermal fluctuation method in air, and (iii) adjusting the deflection sensitivity in solution such that k remains constant. Using this approach, k for the cantilevers was determined to be 2.03 N/m and 2.21 N/m for the LV- and HV-exposure studies, respectively. In addition, the radius of the gold colloidal spheres as measured by scanning electron micrographs was determined to be 3.3 μm and 3.4 μm for the LV and HV exposure studies, respectively. AFM force-displacement measurements included both extension of the cantilever towards the collagen fibril beds and retraction of the cantilever away from the collagen fibril beds with a peak load of 5 nN at a displacement rate of 5.7 μm/s. Force-deformation data were derived from the raw force-displacement measurements by subtracting the cantilever deflection. The unloading portions of the force-deformation curves were analyzed using the Johnson, Kendall, and Roberts (JKR) elastic contact model [44], with the Young's modulus of the fibril bed and the work of adhesion at the fibril bed-probe tip interface as the fitting parameters. A minimum of 14 force-deformation measurements was taken at different locations for each sample. The mean elastic modulus, with the standard deviation, of each sample is reported.

ToF-SIMS of collagen fibril matrices

Collagen matrices formed on Au-coated coverslips were analyzed with an IONTOF IV time-of-flight secondary ion mass spectrometer (IONTOF GmbH, Munster, Germany). Positive- and negative-ion mass spectra were acquired using a pulsed 25 keV Bi_3^+ primary ion source in high current bunched mode, and was rastered randomly over 500 μm × 500 μm areas. Pulsed target current was measured using a Faraday cup and was determined to be 0.04 pA at 10 kHz. Ion dose was kept constant and

at < 10^{12} ions/cm^2 for all analyses, and all ions ranging from m/z= 0 to m/z= 1000 were detected in parallel. A flood gun was used for charge compensation. Positive-ion spectra were mass calibrated using the CH_3^+, $C_2H_3^+$, $C_3H_5^+$, and $C_7H_7^+$ ion fragments before further analysis. Mass calibration of the negative-ion spectra was done using CH^-, O^-, CN^-, and $C_2H_2O^-$ fragments. Minimal spectral features were seen in the negative-ion mode spectra of the matrices, as previously reported for ToF-SIMS analysis of other cellular material (*e.g.*, proteins, lipids, and sugars) [24-29].

Statistical data analysis

Principal component analysis (PCA) was performed on the positive-ion ToF-SIMS data to elucidate any minor spectral differences between the HV-treated and dehydrated fibrils with minimal bias. A comprehensive description of PCA can be found elsewhere [45]. Limiting PCA of the ToF-SIMS data to only amino acid-related fragments, as was suitable in previously reported studies to discriminate between various protein films [15,23,24], could prohibit the identification of glyco-related changes to the surface of the collagen fibrils. Accordingly, all peaks with intensities of at least 100 counts were manually selected. Inorganic-related fragments of Li^+, Na^+, and K^+ were omitted from the spectra, and any spectra with Na^+ intensity greater than 1% of the total ion counts were discarded from the analysis [24,46]. The selected peaks were normalized to the total counts of the all of the selected peaks (average total counts 1.2×10^7 counts ± 0.2×10^7 counts) to account for any differences in secondary ion yields between spectra. The ToF-SIMS data was then arranged in a matrix where the different spectra formed the rows and the individual mass peaks formed the columns. This data matrix was exported to the PLS Toolbox (v.6.2.1 Eigenvector Research, Manson, WA), which was run in MATLAB (v.7.11, MathWorks, Inc., Natick, MA). Lastly, mean-centering the spectra was performed prior to PCA.

Results and discussion

Determining the effect of vacuum exposure on untreated, mechanically compliant collagen fibril matrices

A series of treatments were performed on the collagen matrices prepared as described above. Collagen samples that were immediately stored under PBS at 4°C until further use are referred to as untreated fibril matrices. These have been shown to exhibit mechanical flexibility under the forces imposed by cell spreading and migration [12]. Conversely, passively dehydrated beds of collagen fibrils (referred to as dehydrated fibril matrices) are significantly mechanically stiffer than untreated samples [11,12]. The effects of two other treatments, exposure of untreated matrices to low vacuum (LV-treated) and high vacuum (HV-treated), were analyzed to understand how these conditions affect the properties of previously compliant fibril matrices.

It has been previously observed that adsorbed monomeric proteins denature under HV conditions (*e.g.*, SIMS analysis chamber) [26]. This denaturation results in analytically detectable differences due to conformational changes that result in a display of different surface chemical moieties compared to films that have been chemically stabilized (*e.g.*, trehalose protected, chemically cross-linking, etc.) [23,26,31,32]. If similar conformational changes occur in supramolecular protein structures as compared to their monomeric counterparts, then HV methods for analyzing materials such as decellularized ECMs may likely result in inaccurate determination of biologically relevant mechanical and chemical information. To examine if supramolecular matrix protein assemblies also require stabilization for accurate HV-based analysis, we studied fibrillar collagen matrices, and evaluated them by the biological response they elicited subsequent to HV exposure.

Vascular smooth muscle cells respond to the mechanical characteristics of their ECM in a number of measurable ways [34,40,41], one of which is the extent of cell spreading. We measured the spread area of cells on untreated collagen matrices and compared the results with spreading on matrices that were under HV for 6 h. We found that cells do not spread differently on fibrillar collagen that has experienced HV (Figure 1). Cells on HV-treated fibrils are poorly spread (Figure 1c), much like the cells plated on the untreated fibrils (Figure 1a). As a comparison, cells plated on dehydrated fibrils (Figure 1b) had considerably larger cell areas and noticeably different morphologies. The cell area histogram and mean cell areas (Figure 1d and e, respectively) for the HV-treated fibril matrices (2030 μm^2 ± 137 μm^2) are comparable to the cell areas of untreated fibril matrices measured here (2165 μm^2 ± 206 μm^2) and elsewhere [34]. These results indicate that cells do not sense a difference in the mechanical characteristics of HV-treated collagen fibril matrices compared to untreated matrices. Interesting, cells plated onto collagen fibril matrices that had been LV-treated at pressures of 1 kPa to 10 kPa for 6 h, displayed spreading behavior that was similar to cells on dehydrated matrices (Figure 2), and were significantly more spread than cells on untreated or HV-treated matrices. Cells on LV-treated fibril matrices have larger average surface areas (3450 μm^2 ± 175 μm^2) than the control untreated matrices, and their spread areas are more similar to that of cells plated on dehydrated fibrils (average cell area of 4348 μm^2 ± 287 μm^2). Cell spreading on LV-treated matrices was very similar to what has been observed previously for cells seeded on matrices that have been passively dehydrated for an intermediate time of 4 h [12].

It has been previously shown that the ability of cells to manipulate collagen fibrils affects their spreading response

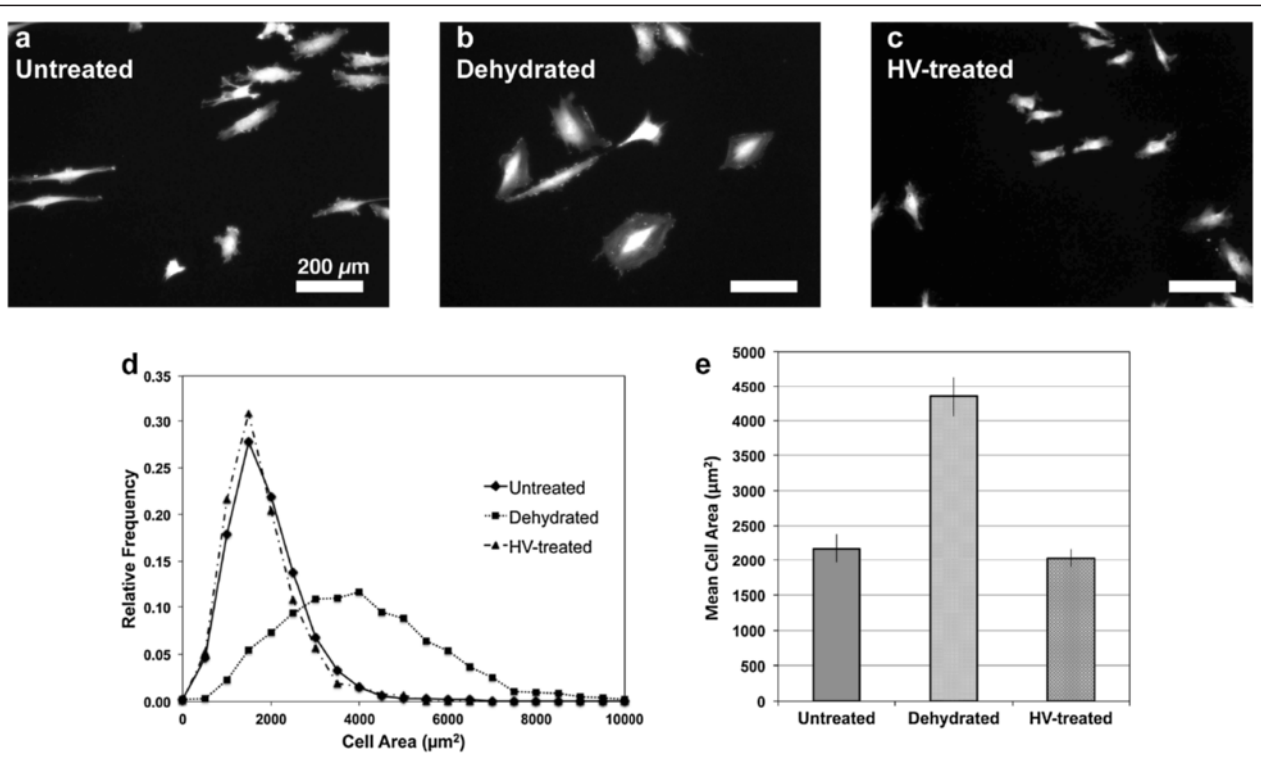

Figure 1 Representative images of A10 vSMCs labeled with Texas Red maleimide after incubation for 24 h on (a) untreated collagen fibril matrices, (b) collagen fibril matrices that have been dehydrated for 24 h, and (c) collagen fibril matrices that have experienced high vacuum (HV, 10^{-7} Pa to 10^{-8} Pa) for approximately 6 h. (d) Histogram of cell areas and **(e)** mean cell areas of A10 vSMC incubated on the different collagen fibril thin matrix states. Image scale bars are 200 μm. Error bars represent the standard deviation of at least three replicate experiments. All samples were made in 50 mm bacterial-grade polystyrene dishes as previously described [34,37].

[12]. As fibrils become more closely packed, as is occurring during the dehydration process [11], it is believed that interfibril attractive forces increase, which causes a decrease in the mechanical compliance of the fibril bed [12,47]. The elastic modulus of the different fibril beds was measured in PBS using AFM. We first measured the elastic modulus of HV-treated fibril matrices in parallel with a set of untreated and dehydrated matrices (Figure 3). In a study performed at a different time, we measured the elastic modulus of the LV-treated fibril matrices in parallel with a second set of untreated and dehydrated matrices (Figure 4). Using the retraction curves of the force-deformation measurements, we fit the modulus of these fibril matrices using the JKR model, as indicated by the

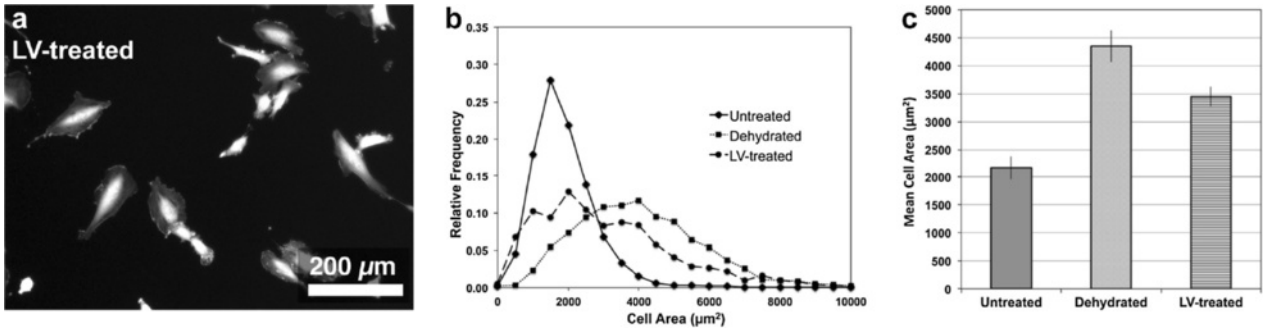

Figure 2 (a) Representative image of A10 vSMCs labeled with Texas Red maleimide after incubation for 24 h on collagen fibril matrices that have experienced low vacuum (LV, 1 kPa to 10 kPa) for approximately 6 h. (b) Histogram of cell areas and **(c)** mean cell areas of A10 vSMC incubated on untreated, dehydrated (both from Figure 1), and LV-treated collagen fibril matrices. Image scale bar is 200 μm. Error bars represent the standard deviation of at least three replicate experiments. All samples were made in 50 mm bacterial-grade polystyrene dishes as previously described [34,37].

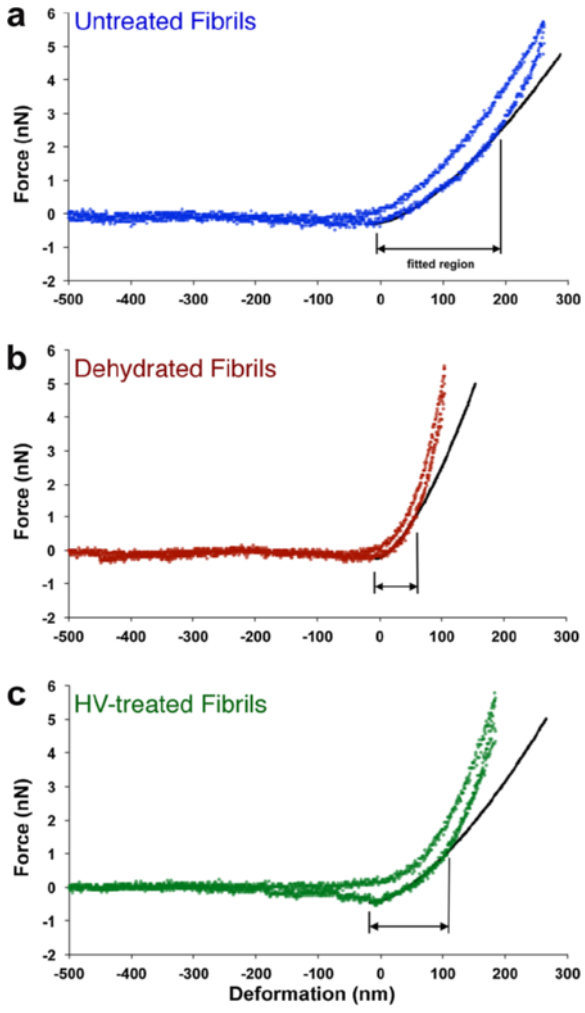

Figure 3 Representative force-deformation curves of the (a) untreated, (b) dehydrated, and (c) HV-treated collagen fibril matrices. Force-deformation curves were obtained using commercially available gold colloidal probe cantilevers at a normal force of 5 nN in PBS at ambient temperature. Black solid lines with the average fit range on the force-deformation curves illustrate the regions fitted to the JKR model to calculate the elastic modulus values for the collagen fibril matrices [11,44]. All samples were made in 50 mm bacterial grade polystyrene dishes as previously described [34,37].

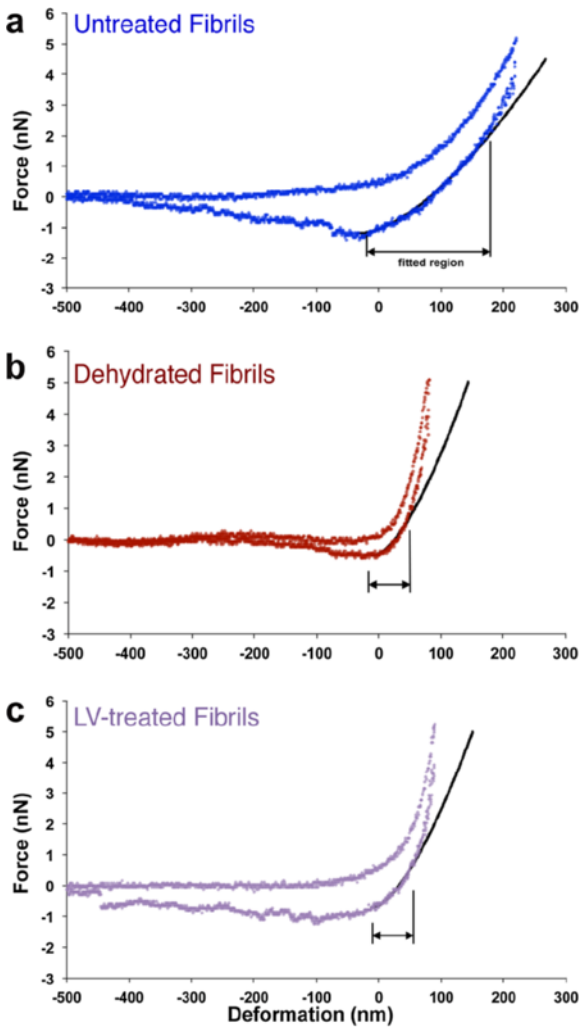

Figure 4 Representative force-deformation curves of the (a) untreated, (b) dehydrated, and (c) LV-treated collagen fibril matrices. Force-deformation curves were obtained using commercially available gold colloidal probe cantilevers at a normal force of 5 nN in PBS at ambient temperature. Black solid lines with the average fit range on the force-deformation curves illustrate the regions fitted to the JKR model to calculate the elastic modulus values for the collagen fibril matrices [11,44]. All samples were made in 50 mm bacterial grade polystyrene dishes as previously described [34,37].

solid black lines in Figures 3 and 4 [11,44]. The modulus results for the first analysis (Table 1) reveal that HV treatment of the fibrils leads to a small, but statically significant ($p < 0.0001$), increase in mechanical rigidity of the fibril matrices. Untreated matrices had a modulus of 8.1 kPa ± 2.2 kPa and HV-treated matrices had a modulus of 13.1 kPa ± 3.8 kPa. However, the HV-treated matrices are approximately a factor of three more compliant than the dehydrated fibril matrices (35.4 kPa ± 4.9 kPa). The modulus results for the second analysis (Table 2) indicate that LV-treated fibril matrices (34.7 kPa ± 3.7 kPa) are nearly as mechanically stiff ($p= 0.20$) as the dehydrated matrices (36.4 kPa ± 4.2 kPa), and are considerably less compliant than the untreated matrices (11.2 kPa ± 3.7 kPa) in this experiment. Variation between the measured modulus values of the two sets of untreated and dehydrated fibril matrices measured here could be attributed to tip-to-tip and instrumental variations. Nevertheless, they are in very close agreement with one another, and with previous measured values of 16 kPa ± 4 kPa and 50 kPa ± 10 kPa, respectively [11].

We hypothesize the differences in mechanical compliance between LV-treated and HV-treated fibril matrices is due to the rate at which interstitial water is removed from between the collagen fibrils. Water surface tension has

Table 1 Measured elastic modulus values of the untreated, dehydrated, and HV-treated collagen fibril matrices.

Fibril Matrix Condition	Elastic Modulus (kPa)
Untreated	8.1 ± 2.2
Dehydrated	35.4 ± 4.9
HV-Exposed	13.1 ± 3.8

Measurements were performed with colloidal probe cantilevers as previously described, and force-deformation curves were fit using the JKR model [11,44]. All samples were made in 50 mm bacterial grade polystyrene dishes as previously described [34,37]. At least 14 different force-deformation measurements were taken for each sample, and the mean values and standard deviations are reported.

been long known to alter sample morphologies for soft samples imaged in a HV environment [28,30,48]. Approaches such as critical point drying or freeze-drying are utilized to prevent malleable, or high aspect ratio structures from collapsing due to capillary forces during water removal [48-50]. In the case of the collagen fibril matrices, the small amount of water that exists between the fibrils in the untreated preparation is expected to be vaporized relatively quickly in the HV environment. Rapid removal of water would minimize the occurrence of capillary forces that can pull the fibrils to one another during a slow drying process, such as apparently occurs under LV. In the LV environment, where pressures are slightly above the vapor pressure of water (2.8 kPa at 23°C), interstitial water is expected to be removed less quickly from the surface. This process is analogous to the ambient dehydration process. Once capillary forces pull the fibrils to one another, this could cause the fibrils to become pinned together resulting in a less compliant matrix [11,12,47]. This drying process presents itself in an observable change in fibril topography, which can be seen in Figure 5 and elsewhere [11]. Line scans of the AFM images of dehydrated and HV-treated fibril matrices (Figure 5b and c) show that the average large fibril heights were 132 nm ± 5 nm and 181 nm ± 16 nm, respectively. These values follow the same trend seen we have observed previously, where the height of large untreated fibrils decreased as a result of dehydration (from 147 nm ± 18 nm for untreated samples to 118 nm ± 15 nm for dehydrated samples) [11]. By no means do we suggest HV is an ideal method for rapidly removing water interstitially in high aspect ratio thin films to reduce capillary forces, but it is effective enough not to significantly change the compliance or bioactivity of these fibril matrices, at least as detectable within the sensitivity of these measurements.

Table 2 Measured elastic modulus values of the untreated, dehydrated, and LV-treated collagen fibril matrices.

Fibril Matrix Condition	Elastic Modulus (kPa)
Untreated	11.2 ± 3.7
Dehydrated	36.4 ± 4.2
LV-Exposed	34.7 ± 3.7

Measurements were performed with colloidal probe cantilevers as previously described, and force-deformation curves were fit using the JKR model [11,44]. All samples were made in 50 mm bacterial grade polystyrene dishes as previously described [34,37]. At least 14 different force-deformation measurements were taken for each sample, and the mean values and standard deviations are reported.

Elucidating ToF-SIMS spectral differences of mechanically modulated collagen fibril matrices

ToF-SIMS is an increasingly popular analytical method for studying decellularized and acellular ECMs [14,15,21]. A strength of ToF-SIMS is that it can provide insights into spectral differences that may arise as result from structural changes in ECM samples. We used ToF-SIMS to examine untreated and dehydrated collagen fibril matrices to see if any detectable changes in matrix structure occur as a result of dehydration. The data in Figure 3 and Table 1 establishes that exposure to a HV environment did not significantly affect the mechanical properties of compliant collagen fibril matrices, which corroborates the data in Figure 1 showing that cells did not respond differently to the HV-treated fibrils compared to untreated fibrils. Therefore, ToF-SIMS is an appropriate technique to apply to this question, and we will assume that HV-treated matrices are equivalent to untreated matrices. However, even though we are comparing the ToF-SIMS data from untreated and dehydrated matrices, for the subsequent results shown and discussed we do refer to untreated matrices as HV-treated, because technically they were exposed to HV for ToF-SIMS analysis. It would be disingenuous to call these samples 'untreated', even if they retained the same bioactive and mechanical properties.

Representative positive-ion mass spectra of HV-treated and dehydrated fibril matrices are shown in Figure 6. No noticeable spectral differences were observed between the different matrices. Representative negative-ion spectra (Additional file 1: Figure S1) also showed minimal spectral differences between the two samples. As a control, we found that the cell response to these samples, post-ToF-SIMS analysis, were similar to what we established previously (Figure 1), where HV-treated matrices retained the bioactivity of untreated collagen fibrils as indicated by the cell area histogram and mean cell area (Additional file 1: Figure S2). These results (Additional file 1: Figure S2) illustrate the robustness of these matrices, which remain unaffected by HV exposure regardless of whether the collagen fibrils are formed on polystyrene or on alkanethiol-modifed gold substrates.

PCA was used to reveal subtle spectral differences in the positive-ion spectra between the HV-treated and dehydrated fibril matrices. No further analysis was performed on the negative-ion spectra due to the lack of spectral information it provides, which has also been

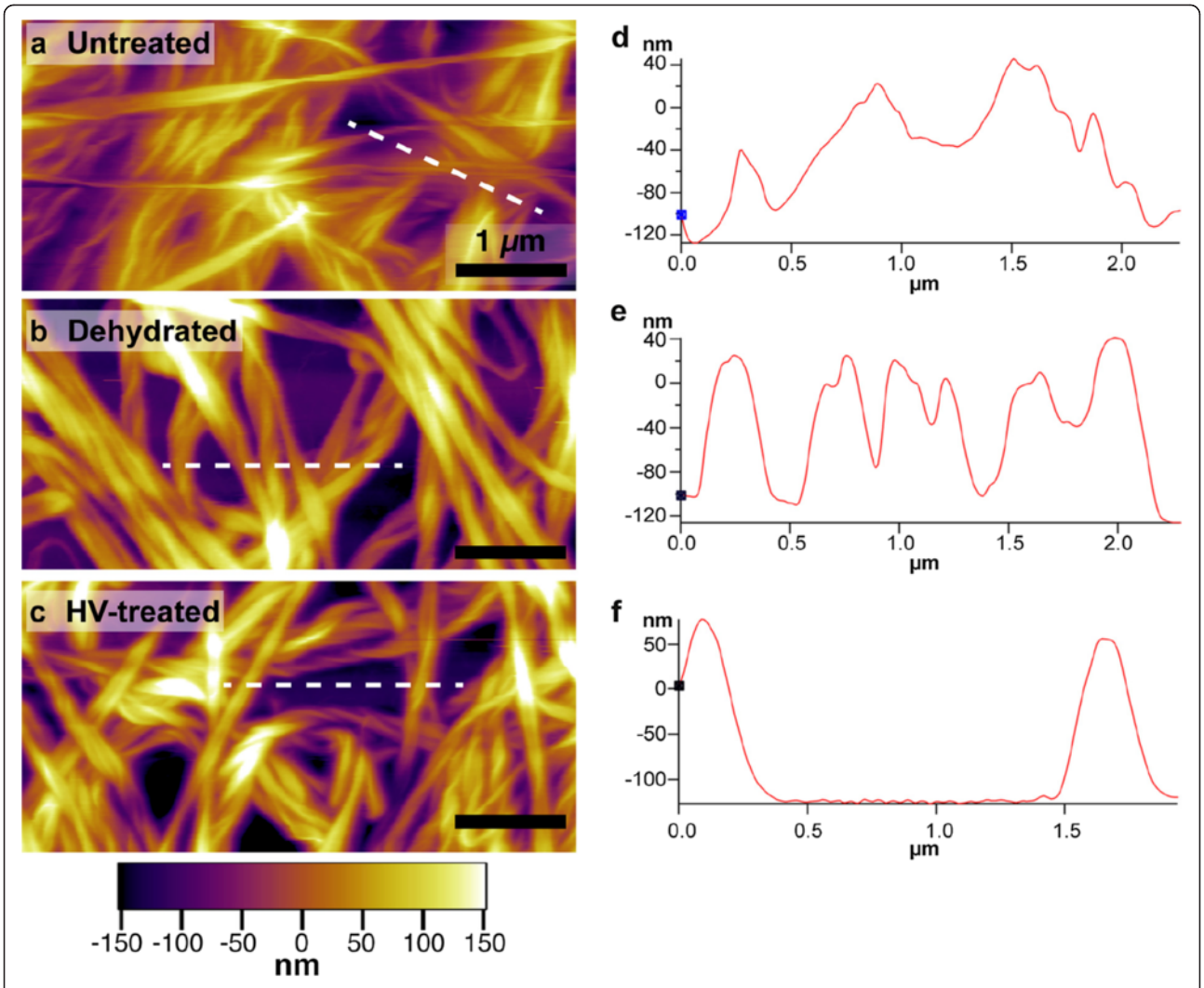

Figure 5 Representative AFM topography images of the (a) untreated, (b) dehydrated, and (c) HV-treated collagen fibril matrices. The representative line scans of the untreated, dehydrated, and HV-treated collagen fibril matrices (**d-f**, respectively) are indicated by the dashed white lines in the respective AFM images. AFM images were acquired in intermittent-contact mode over a 5 μm × 5 μm area at a linear scan rate of 0.18 Hz to 0.3 Hz with silicon nitride probes in PBS at ambient temperature.

observed in the ToF-SIMS analysis of other biologically relevant samples [15,24-27,29]. Statistically significant spectral variance between the fibril matrix states was captured in the first principal component (PC1) as seen in Figure 7a, where the 95% confidence ellipses for both samples never intersect one another in the scores plot. Examination of the loadings plot seen in Figure 7b (Additional file 1: Table S1 identifies these fragments with their corresponding loading values) suggests that discrimination is based on differences in relative intensities of small fragments compared to larger molecular fragments. Here, small mass peaks with m/z approximately less than 73 load positively on PC1 (Figure 7b), which correlates with the dehydrated fibril spectral data with positive scores on PC1 (Figure 7a). These data suggest that compared to untreated matrices, dehydrated matrices show a greater relative abundance of these small fragments compared to larger fragments with m/z approximately greater than 73. The opposite is true for untreated matrices that have negative scores on PC1 (Figure 7a), which correlates with the negative loadings of fragments of m/z approximately greater than 73 on PC1 (Figure 7b). This indicates that the ToF-SIMS data of untreated samples has a greater relative abundance of larger mass fragments compared to small mass fragments than the data for the dehydrated matrices. It should be noted that we did not detect the appearance of any new fragments, or the disappearance of any fragments due to the dehydration process. Additional file 1: Figure S3 shows that the ToF-SIMS results were reproducible. The results of this analysis were confirmed by PCA analysis that was limited to an established set of amino acid-

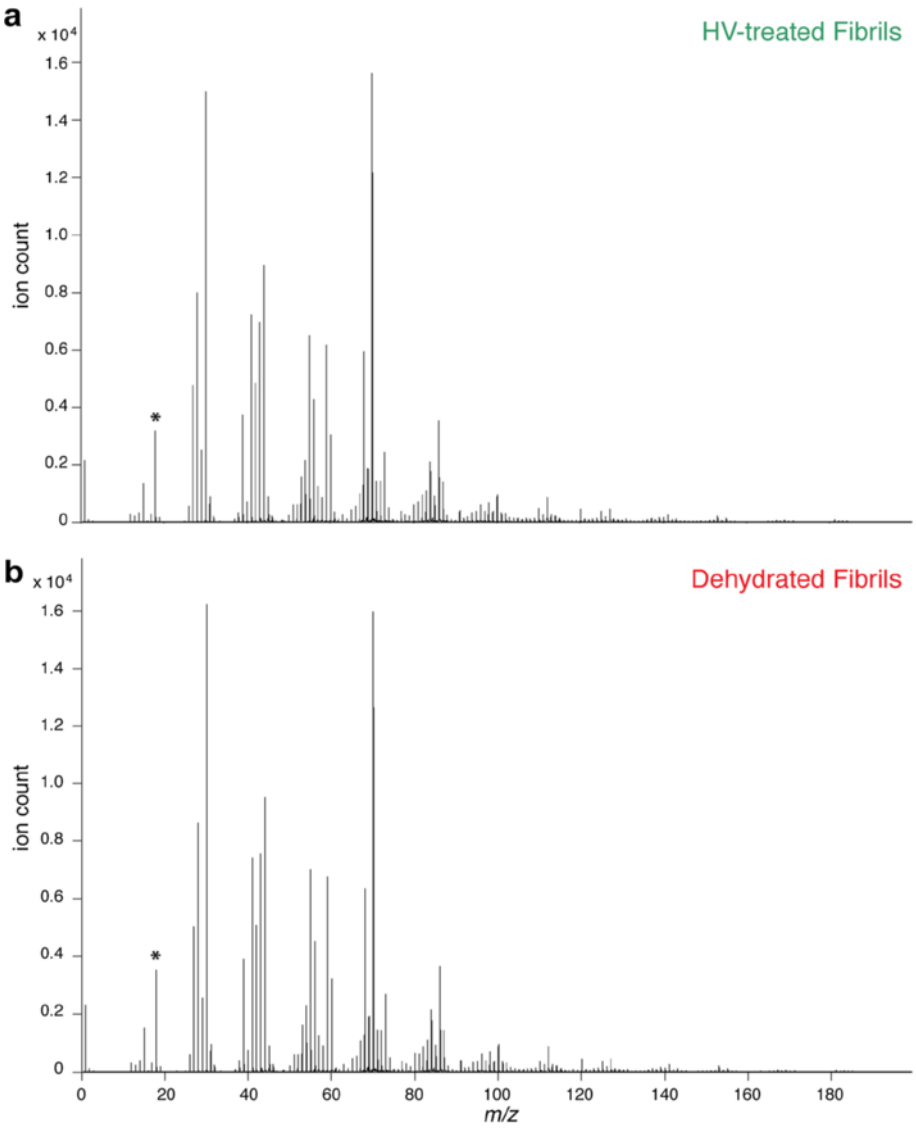

Figure 6 Representative positive-ion ToF-SIMS spectra of (a) HV-treated and (b) dehydrated collagen fibril matrices. Spectra were collected well below the static limit (< 10^{12} ions/cm^2). Spectra were calibrated using the CH_3^+, $C_2H_3^+$, $C_3H_5^+$, and $C_7H_7^+$ fragments. The H_3O^+ is annotated (*) to illustrate that the yields in both samples were similar, and that no signal enhancement due to water was present in the spectrum of the HV-treated fibril matrix. The ion dose was held constant for all samples, and both spectra had total secondary ion counts of approximately 1.2×10^7.

related peaks (Additional file 1: Figure S4) [15]. Such a restricted analysis has been shown to assist in discrimination based on chemically relevant information, and minimize the affects of sample-to-sample variations or contaminations [25,28]. This analysis confirms that discrimination between samples is based on the abundance of small fragments relative to larger molecular fragments, and not due to amino acid changes at the surface of the matrices.

It is unclear what the observed minor differences in spectra between the HV-treated and dehydrated fibril films are due to. One could speculate that the higher relative abundance of large molecular fragments with greater than $m/z \approx 73$ in the HV-treated fibril matrices could be due to enhancement from the presence of water within the wrapped rope-like structure of the collagen fibrils that is not removed in the HV environment. However, signal enhancement due to water is typically accompanied by an increased yield of H_3O^+ [51], which is not present in the positive-ion spectra of the untreated fibril matrices (Figure 6, H_3O^+ signal is annotated). Alternatively, the spectral differences observed here could be due to topographic differences between the two samples. We have shown here and elsewhere [11] that the average

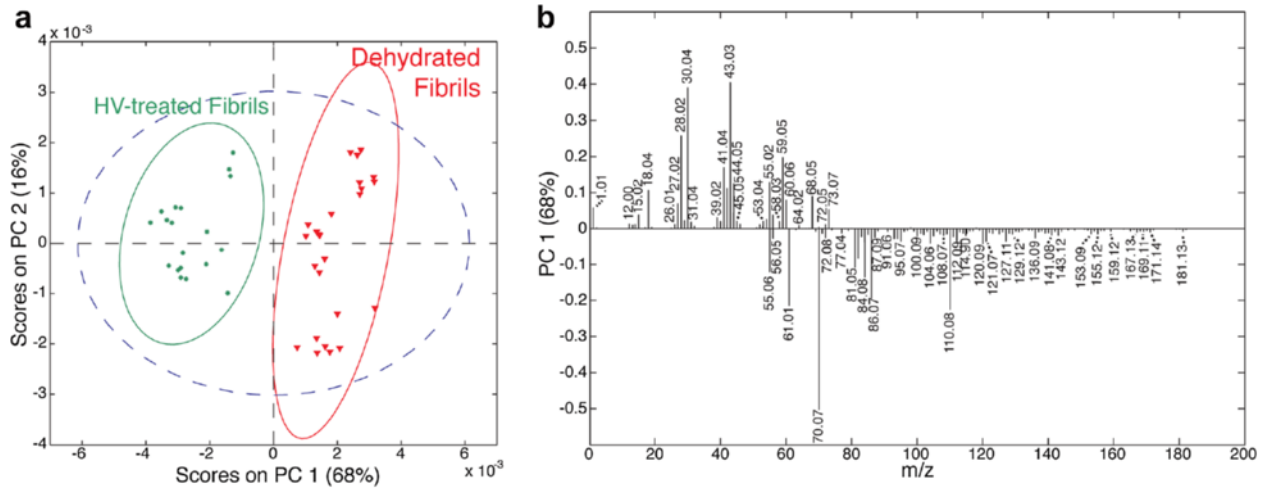

Figure 7 (a) Scores and (b) loading plots from PCA of the ToF-SIMS positive-ion spectra acquired from HV-treated and dehydrated collagen fibril matrices. PCA was performed on all peaks with intensities of at least 100 counts (except Li^+, Na^+, and K^+) to elucidate any minor spectral differences between the HV-treated and dehydrated fibrils, without bias, which may be present as a result in the change of fibrillar matrix state. Peaks were normalized to the total ion counts and mean-centered. The solid line ellipses and the dashed line ellipse represent the 95% confidence limit for each group and the entire PC model, respectively.

height of the large fibrils is reduced during the dehydration process, and it has been established previously that PCA can capture topographical differences in the ToF-SIMS data of samples [52]. Another possibility is that our observations are due to the fact that the dehydration process causes the large fibrils to become brittle [12]. Therefore we may expect to see that the mechanically stiff matrices have relatively higher yields in small m/z fragments than in the mechanically compliant matrices. Differences in topography and/or brittleness may also explain why the H^- yield in the negative-ion spectrum of the dehydrated fibril matrices (Additional file 1: Figure S1b) is larger than in untreated matrices (Additional file 1: Figure S1a). Regardless of what causes the observed increase of small fragments, the ToF-SIMS results indicate there are no measureable chemical changes at the surface of the fibril matrices due to the dehydration process. This is corroborated by our previous work that found known biochemical cues remain intact between the untreated and dehydrated matrix states [36,37].

Conclusions

This work demonstrates that unlike their monomeric protein film counterparts [26,31,32], collagen type I fibril matrices are not mechanically or biochemically altered by the HV environment. Collagen type I is the primary protein in connective tissue [13,38,39], and the supramolecular structures that constitute the fibril matrices in this study are a physiologically relevant configuration of collagen [35]. To the extent that these collagen matrices are similar to the fibrillar structures found in decellularized matrices, these results support the possibility that HV methods can provide accurate information about decellularized ECMs.

Additional file

Additional file 1: Figure S1. Representative negative-ion ToF-SIMS spectra of (**a**) HV-treated and (**b**) dehydrated collagen fibril matrices. Spectra were collected well below the static limit (< 10^{12} ions/cm^2). Spectra were calibrated using the CH^-, O^-, CN^-, and $C_2H_2O^-$ fragments. The ion dose was held constant for all samples. **Figure S2** (**a**) Histogram of cell areas and (**b**) mean cell areas of A10 vSMC incubated on untreated and dehydrated collagen fibril matrices formed on PS dishes (Figure 1) and hexadecane thiol-treated, Au-coated cover slips after ToF-SIMS analysis. Error bars represent the standard deviation of at least three replicate experiments. **Figure S3** Projection of the ToF-SIMS positive-ion spectra acquired from a second set of HV-treated and dehydrated collagen fibril matrices made at a later date onto the PC scores plot of the original data from Figure 7. Post-analysis cell spreading experiments, analogous to those seen in Figure 1 and Additional file 1: Figure S1, of the second set of fibril matrices indicated that the HV environment did not affect cell responses of the compliant fibril matrices (data not shown). The black dashed lines and the colored dashed lines represent the 95% confidence limit for the entire PC model and each group, respectively. **Figure S4** (**a**) Scores and (**b**) loading plots from PCA of the ToF-SIMS positive-ion spectra acquired from HV-treated and dehydrated collagen fibril matrices. PCA was performed using the amino acid-related peak set previously described [1] to elucidate any minor spectral differences due to protein conformational changes, which maybe present as a result in the change of state of fibrillar collagen. Peaks were normalized to the total ion counts and mean-centered. The solid line ellipses and the dashed line ellipse represent the 95% confidence limit for each group and the entire PC model, respectively. **Table S1** Loadings values from PCA of the ToF-SIMS positive-ion spectra acquired from HV-treated and dehydrated collagen fibril matrices performed on all peaks (Figure 7b). Only loadings with weights of at least a hundredth of a factor are shown for brevity (**Peaks used for spectra calibration). **Table S2** Loadings values from PCA of the ToF-SIMS positive-ion spectra acquired from HV-treated and dehydrated collagen fibril matrices performed using only the amino acid-related fragments [1].

Competing interests
The author(s) declare that they have no competing interests.

Authors' contributions
CRA: design of experiments, participated in all data collection and analysis, and drafted the manuscript; FWD: force-displacement measurements and analysis; KB: protocols for collagen fibril matrices, cell staining and microscopy; ALP: experimental design, data reduction and analysis.
All authors read and approved the final manuscript.

Supporting information available
Figures illustrating the representative negative-ion spectra of the HV-treated and dehydrated matrices, cell spreading on the ToF-SIMS analyzed samples, and PCA using an amino acid-related peak set of the ToF-SIMS positive-ion spectra of HV-treated and dehydrated fibril matrices. Also, tables summarizing the loading values for each PCA of the positive-ion ToF-SIMS data. This material is available free of charge on the Internet.

Acknowledgments
The authors would like to thank Dr. Karen T. Henry for assisting in the SEM measurements to determine the radii of the AFM colloidal probes. Furthermore, the authors would like to thank Dr. John T. Elliot, Dr. Christopher Szakal, and Dr. Shin Muramoto for useful discussions. CRA was supported by the National Research Council Associates Program.

Author details
[1]Material Measurement Laboratory, National Institute of Standards and Technology, Gaithersburg, MD 20899, USA. [2]Fischell Department of Bioengineering, University of Maryland, College Park, MD 20742, USA.

Received: 6 December 2012 Accepted: 17 January 2013
Published: 17 January 2013

References

1. Holly SP, Larson MK, Parise LV (2000) Multiple roles of integrins in cell motility. Exp Cell Res 261(1):69–74
2. Dallas SL, Chen Q, Sivakumar P (2006) Dynamics of assembly and reorganization of extracellular matrix proteins. Curr Top Dev Biol 75:1–24. http://www.ncbi.nlm.nih.gov/pubmed/16984808
3. Roskelley CD, Bissell MJ (2002) The dominance of the microenvironment in breast and ovarian cancer. Semin Cancer Biol 12(2):97–104
4. McCloskey KE, Gilroy ME, Nerem RM (2005) Use of embryonic stem cell-derived endothelial cells as a cell source to generate vessel structures *in vitro*. Tissue Eng 11(3–4):497–505
5. Mercier I, Lechaire J-P, Desmouliere A, Fo G, Aumailley M (1996) Interactions of human skin fibroblasts with monomeric or fibrillar collagens induce different organization of the cytoskeleton. Exp Cell Res 225(2):245–256
6. Hynes RO (2002) Integrins: bidirectional, allosteric signaling machines. Cell 110(6):673–687
7. Lo C-M, Wang H-B, Dembo M, Y-l W (2000) Cell movement is guided by the rigidity of the substrate. Biophys J 79(1):144–152
8. Plant AL, Bhadriraju K, Spurlin TA, Elliott JT (2009) Cell response to matrix mechanics: focus on collagen. BBA-Mol Cell Res 1793(5):893–902
9. Lathia JD, Rich JN (2012) Holding on to stemness. Nat Cell Biol 14(5):450–452
10. Trappmann B, Gautrot JE, Connelly JT, Strange DGT, Li Y, Oyen ML, Cohen Stuart MA, Boehm H, Li B, Vogel V, Spatz JP, Watt FM, Huck WTS (2012) Extracellular-matrix tethering regulates stem-cell fate. Nat Mater 11(7):642–649
11. Chung K-H, Bhadriraju K, Spurlin TA, Cook RF, Plant AL (2010) Nanomechanical properties of thin films of type I collagen fibrils. Langmuir 26(5):3629–3636
12. McDaniel DP, Shaw GA, Elliott JT, Bhadriraju K, Meuse C, Chung K-H, Plant AL (2007) The stiffness of collagen fibrils influences vascular smooth muscle cell phenotype. Biophys J 92(5):1759–1769
13. Badylak SF, Freytes DO, Gilbert TW (2009) Extracellular matrix as a biological scaffold material: structure and function. Acta Biomater 5(1):1–13
14. Barnes CA, Brison J, Michel R, Brown BN, Castner DG, Badylak SF, Ratner BD (2011) The surface molecular functionality of decellularized extracellular matrices. Biomaterials 32(1):137–143
15. Canavan HE, Graham DJ, Cheng X, Ratner BD, Castner DG (2006) Comparison of native extracellular matrix with adsorbed protein films using secondary ion mass spectrometry,Ä†. Langmuir 23(1):50–56
16. Yeung T, Georges PC, Flanagan LA, Marg B, Ortiz M, Funaki M, Zahir N, Ming W, Weaver V, Janmey PA (2005) Effects of substrate stiffness on cell morphology, cytoskeletal structure, and adhesion. Cell Motil Cytoskel 60(1):24–34
17. Gilbert TW, Sellaro TL, Badylak SF (2006) Decellularization of tissues and organs. Biomaterials 27(19):3675–3683
18. Hsiao Y-C, Lee H-W, Chen Y-T, Young T-H, Yang T-L (2011) The impact of compositional topography of amniotic membrane scaffold on tissue morphogenesis of salivary gland. Biomaterials 32(19):4424–4432
19. Canavan HE, Cheng X, Graham DJ, Ratner BD, Castner DG (2004) Surface characterization of the extracellular matrix remaining after cell detachment from a thermoresponsive polymer. Langmuir 21(5):1949–1955
20. Ott HC, Matthiesen TS, Goh S-K, Black LD, Kren SM, Netoff TI, Taylor DA (2008) Perfusion-decellularized matrix: using nature's platform to engineer a bioartificial heart. Nat Med 14(2):213–221
21. Brown BN, Barnes CA, Kasick RT, Michel R, Gilbert TW, Beer-Stolz D, Castner DG, Ratner BD, Badylak SF (2010) Surface characterization of extracellular matrix scaffolds. Biomaterials 31(3):428–437
22. Klerk LA, Dankers PYW, Popa ER, Bosman AW, Sanders ME, Reedquist KA, Heeren RMA (2010) TOF-secondary Ion mass spectrometry imaging of polymeric scaffolds with surrounding tissue after *in vivo* implantation. Anal Chem 82(11):4337–4343
23. Baugh L, Weidner T, Baio JE, Nguyen P-CT, Gamble LJ, Stayton PS, Castner DG (2010) Probing the orientation of surface-immobilized protein G B1 using ToF-SIMS, sum frequency generation, and NEXAFS spectroscopy. Langmuir 26(21):16434–16441
24. Wagner MS, Castner DG (2001) Characterization of adsorbed protein films by time-of-flight secondary ion mass spectrometry with principal component analysis. Langmuir 17:4649–4660
25. Wagner MS, Tyler BJ, Castner DG (2002) Interpretation of static time-of-flight secondary ion mass spectra of adsorbed protein films by multivariate pattern recognition. Anal Chem 74:1824–1835
26. Xia N, May CJ, McArthur SL, Castner DG (2002) Time-of-flight secondary Ion mass spectrometry analysis of conformational changes in adsorbed protein films. Langmuir 18(10):4090–4097
27. Berman ESF, Kulp KS, Knize MG, Wu L, Nelson EJ, Nelson DO, Wu KJ (2006) Distinguishing monosaccharide stereo- and structural isomers with TOF-SIMS and multivariate statistical analysis. Anal Chem 78(18):6497–6503
28. Anderton CR, Vaezian B, Lou K, Frisz JF, Kraft ML (2011) Identification of a lipid-related peak set to enhance the interpretation of TOF-SIMS data from model and cellular membranes. Surf Interface Anal 44(3):322–333
29. Vaezian B, Anderton CR, Kraft ML (2010) Discriminating and imaging different phosphatidylcholine species within phase-separated model membranes by principal component analysis of TOF-secondary Ion mass spectrometry images. Anal Chem 82(24):10006–10014
30. Kulp KS, Berman ESF, Knize MG, Shattuck DL, Nelson EJ, Wu L, Montgomery JL, Felton JS, Wu KJ (2006) Chemical and biological differentiation of three human breast cancer cell types using time-of-flight secondary Ion mass spectrometry. Anal Chem 78(11):3651–3658
31. Xia N, Castner DG (2003) Preserving the structure of adsorbed protein films for time-of-flight secondary ion mass spectrometry analysis. J Biomed Mater Res A 67A(1):179–190
32. Xia N, Shumaker-Parry JS, Zareie MH, Campbell CT, Castner DG (2004) A streptavidin linker layer that functions after drying. Langmuir 20(9):3710–3716
33. Elliott JT, Halter M, Plant AL, Woodward JT, Langenbach KJ, Tona A (2008) Evaluating the performance of fibrillar collagen films formed at polystyrene surfaces as cell culture substrates. Biointerphases 3(2):19–28
34. Elliott JT, Tona A, Woodward JT, Jones PL, Plant AL (2003) Thin films of collagen affect smooth muscle cell morphology. Langmuir 19(5):1506–1514
35. Meshel AS, Wei Q, Adelstein RS, Sheetz MP (2005) Basic mechanism of three-dimensional collagen fibre transport by fibroblasts. Nat Cell Biol 7(2):157–164
36. Bhadriraju K, Chung K-H, Spurlin TA, Haynes RJ, Elliott JT, Plant AL (2009) The relative roles of collagen adhesive receptor DDR2 activation and matrix stiffness on the downregulation of focal adhesion kinase in vascular smooth muscle cells. Biomaterials 30(35):6687–6694

37. Spurlin TA, Bhadriraju K, Chung K-H, Tona A, Plant AL (2009) The treatment of collagen fibrils by tissue transglutaminase to promote vascular smooth muscle cell contractile signaling. Biomaterials 30(29):5486–5496
38. Di Lullo GA, Sweeney SM, Korkko J, Ala-Kokko L, San Antonio JD (2002) Mapping the ligand-binding sites and disease-associated mutations on the most abundant protein in the human, type I collagen. J Biol Chem 277(6):4223–4231
39. Nimni ME (1988) Collagen. CRC, Boca Raton, FL. http://www.amazon.com/Collagen-Biochemistry-Vol-Marcel-Nimni/dp/0849346010
40. Elliott JT, Woodward JT, Langenbach KJ, Tona A, Jones PL, Plant AL (2005) Vascular smooth muscle cell response on thin films of collagen. Matrix Biol 24(7):489–502
41. Langenbach K, Elliott J, Tona A, McDaniel D, Plant A (2006) Thin films of type 1 collagen for cell by cell analysis of morphology and tenascin-C promoter activity. BMC Biotechnol 6(1):14
42. Elliott JT, Tona A, Plant AL (2003) Comparison of reagents for shape analysis of fixed cells by automated fluorescence microscopy. Cytometry A 52A (2):90–100
43. Ducker WA, Senden TJ, Pashley RM (1991) Direct measurement of colloidal forces using an atomic force microscope. Nature 353(6341):239–241
44. Johnson KL, Kendall K, Roberts AD (1971) Surface Energy and the Contact of Elastic Solids. Proc London R Soc A-Math Phys Eng Sci 324(1558):301–313
45. Wold S (1987) Principal component analysis. Chemom Intell Lab Syst 2:37–52
46. Oran U, Unveren E, Wirth T, Unger WES (2004) Poly-dimethyl-siloxame (PDMS) contamination of polystyrene (PS) oligomers samples: a comparison of time-of-flight static secondary ion mass spectrometry (TOF-SSIMS) and X-ray photoelectron spectroscopy (XPS) results. Appl Sur Sci 227:318–324
47. Rosenblatt J, Devereux B, Wallace DG (1994) Injectable collagen as a pH-sensitive hydrogel. Biomaterials 15(12):985–995
48. Szakal C, Narayan K, Fu J, Lefman J, Subramaniam S (2011) Compositional mapping of the surface and interior of mammalian cells at submicrometer resolution. Anal Chem 83(4):1207–1213
49. Duan H, Berggren KK (2010) Directed self-assembly at the 10 nm scale by using capillary force-induced nanocohesion. Nano Lett 10(9):3710–3716
50. Jeon S, Park J-U, Cirelli R, Yang S, Heitzman CE, Braun PV, Kenis PJA, Rogers JA (2004) Fabricating complex three-dimensional nanostructures with high-resolution conformable phase masks. Proc Natl Acad Sci USA 101(34):12428–12433
51. Chandra S (2008) Challenges of biological sample preparation for SIMS imaging of elements and molecules at subcellular resolution. Appl Surf Sci 255(4):1273–1284
52. Pachuta SJ (2004) Enhancing and automating TOF-SIMS data interpretation using principal component analysis. Appl Sur Sci 231–232:217–223

doi:10.1186/1559-4106-8-2
Cite this article as: Anderton *et al.*: **The effect of high vacuum on the mechanical properties and bioactivity of collagen fibril matrices.** *Biointerphases* 2013 **8**:2.